

DYNAMIC PERFORMANCE OPTIMIZATION OF SHUNT ACTIVE POWER FILTER TO ELIMINATE TOTAL HARMONIC DISTORTION

Abdelmoezz Ahmed Eid^{1*}, Ahmed Mohammed Attiya Soliman¹, Mohammed A. Mehanna¹

¹ Electrical Engineering Department, Faculty of Engineering, Al-Azhar University, Cairo, Egypt.

*Correspondence: engabdelmoezz@azhar.edu.eg

Received: 5 Nov. 2022 Accepted: 28 Dec. 2022

ABSTRACT

In this paper, a proposed efficient solution for an important power quality problem focused on harmonic distortion in the source current is introduced by using Shunt Active Power Filter (SAPF) controlled by the sinusoidal source current control strategy which is based on the instantaneous active and reactive power theory (Sinusoidal PQ-theory). As a part of this controller, there is PI-Controller which enhances the APF controller performance when tuning its proportional and integral gains. The gains of the PI-Controller are optimized in this article based on an effective metaheuristic optimization algorithm known as Mayfly Optimization Algorithm (MOA), and its effectiveness is clear when compared with other algorithms such as Particle Swarm Optimization (PSO), Artificial Hummingbird Algorithm (AHA) and Archimedes Optimization Algorithm (AOA). The performance of the optimized controller is evaluated under load variation and distorted source voltage conditions. The results obtained using MATLAB/SIMULINK prove the ability of the MOA to get the optimal PI-Controller gains which lead to enhancement of the APF controller performance to reduce the total harmonic distortion in the drawing source current with minimum and acceptable values according to (IEEE-519) harmonics standard.

KEYWORDS: Power Quality; Total Harmonic Distortion; Shunt Active Power Filter; PI-Controller Tuning; Mayfly Optimization Algorithm.

تحسين الأداء الديناميكي لمرشح الطاقة النشط المتصل على التوازي لإزالة التشوه التوافقي الكلي

عبدالمعز أحمد عيد محمد^{1*}، أحمد محمد عطية سليمان¹، محمد أحمد أحمد مهنى¹

¹ قسم الهندسة الكهربائية، كلية الهندسة، جامعة الأزهر، القاهرة، مصر

البريد الإلكتروني: engabdelmoezz@azhar.edu.eg

المخلص

في هذا البحث، تم تقديم مقترح بحل فعال لمشكلة مهمة تتعلق بجودة الطاقة تركز على التشويه التوافقي (HD) باستخدام مرشح القدرة نشط (APF) يتم التحكم فيه بواسطة استراتيجية التحكم في تيار المصدر الجيبي والتي تعتمد على نظرية القدرة الفعالة وغير الفعالة اللحظية (Sinusoidal PQ-Theory). كجزء من وحدة التحكم، توجد وحدة تحكم PI-Controller تقوم بتعزيز أداء وحدة التحكم في مرشح القدرة النشط APF عند ضبط مكاسبه النسبية والتكاملية. تم تحسين مكاسب وحدة التحكم PI-Controller في هذه الورقة البحثية بناءً على خوارزمية تحسين فعالة تُعرف باسم خوارزمية ذبابة مايو (MOA)، وتكون فعاليتها واضحة عند مقارنتها بالخوارزميات الأخرى مثل خوارزمية سرب الجسيمات (PSO)،

DYNAMIC PERFORMANCE OPTIMIZATION OF SHUNT ACTIVE POWER FILTER TO ELIMINATE TOTAL HARMONIC DISTORTION

وخوارزمية الطائر الطنان الاصطناعي (AHA) وخوارزمية تحسين أرشميدس (AOA). يتم تقييم أداء وحدة التحكم المُحسَّنة في ظل تغير الحمل وظروف تشوه جهد المصدر. أثبتت النتائج التي تم الحصول عليها باستخدام MATLAB/SIMULINK قدرة MOA على الحصول على مكاسب PI-Controller المثلى والتي تؤدي إلى تحسين أداء وحدة التحكم APF لتقليل التشوه التوافقي الكلي في تيار مصدر الرسم مع قيم صغيرة ومقبولة وفقاً للمواصفات القياسية (IEEE -519) الخاصة بالتوافقيات.

الكلمات المفتاحية: نوعية الطاقة؛ مجموع التشويه التوافقي؛ مرشح الطاقة النشط؛ ضبط تنعيم وحدة التحكم PI؛ خوارزمية Mayfly.

1. INTRODUCTION

Because of the rapid advancement of power electronics technology, which has undoubtedly resulted in the widespread use of non-linear loads, maintaining the level of total harmonic distortion (THD) of a power source within the permissible limit as defined by the IEEE 519 [1] standard has become extremely difficult. During operation, these non-linear loads introduce harmonic currents into the power system, decreasing the power quality by increasing the THD value, decreasing the overall system efficiency, and potentially causing other problems associated with equipment failure due to overheating [2-4]. As a result, attempts are needed to reduce the harmful effects of these harmonic currents and ultimately keep them within an acceptable level. Several mitigation techniques were put in place, the most notable of which was the invention of shunt active power filters (SAPFs), which are effective against harmonic current issues [5, 6]. As shown in Fig. 1, The SAPF configuration is made up of two major components : the active filter controller and the voltage source inverter (VSI). The controller oversees selecting suitable instantaneous firing signals, which are constantly transmitted to the VSI, which injects a regulated compensating current into the power system [7]. During operation, a typical SAPF will first measure the harmonic contents of the harmonic fusing power system, and based on this measurement, the SAPF will create a compensating current to be injected back into the power system for mitigating the harmonic currents existing in the power system. It is vital to highlight that mitigation is deemed successful when the supply current can restore its sinusoidal form with a THD value of 5% or less [1], runs in phase, and has the same fundamental frequency as the source voltage [8, 9].

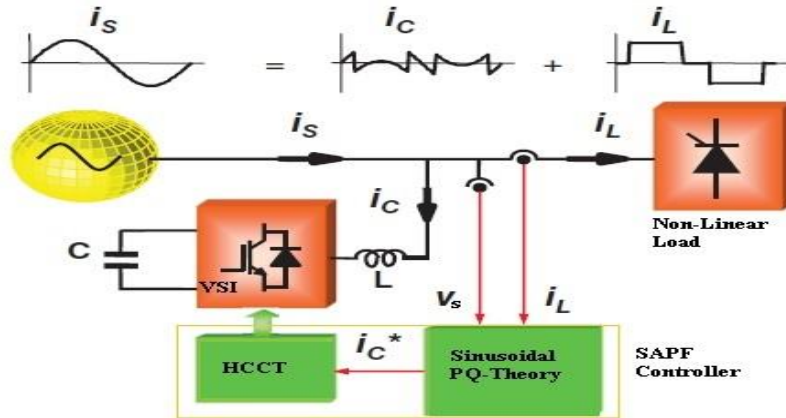


Fig. 1: Configuration of the SAPF [10].

2. PROPOSED CONTROLLER OF SAPF

No matter how dependable a SAPF is, it cannot work correctly without a proper and precisely built control system, which typically includes control stages such as harmonic data extraction, DC link voltage regulation, power system synchronization, and control pulse generation. The extraction of harmonic data is the first stage and has been identified as the most critical stage [11]. As a result, implementing all the other associated control phases would be pointless without the required harmonic data for the power system. There are various technologies accessible today, and many efforts have been made to categorize them based on the time

DYNAMIC PERFORMANCE OPTIMIZATION OF SHUNT ACTIVE POWER FILTER TO ELIMINATE TOTAL HARMONIC DISTORTION

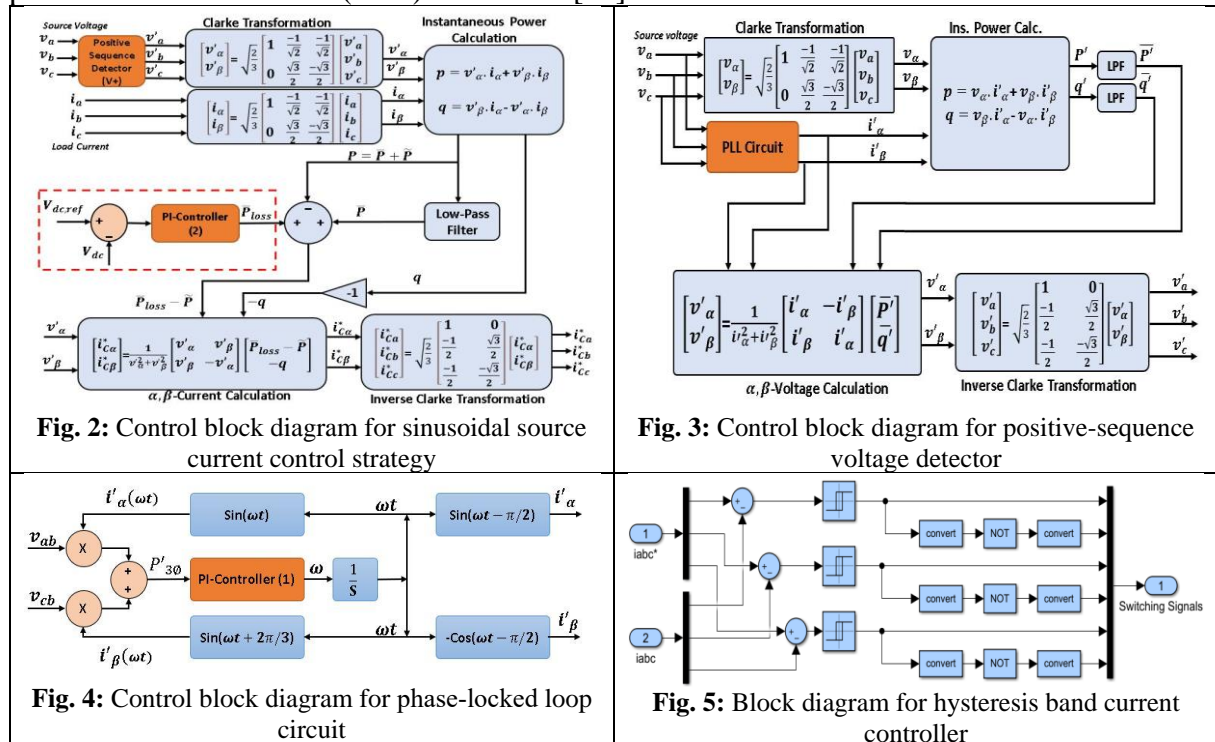
domain, frequency domain, and learning methodologies [12]. Reference generation theories or control techniques are used to examine VSI switching. SAPF control strategies may be used in two stages: extracting compensating signals from distorted signals using reference current-generation theories and creating suitable firing signals to control the SAPF switches using the signal's estimated reference methods [13].

2.1. The sinusoidal source current control strategy (Sinusoidal PQ-theory)

The instantaneous active and reactive power theory (PQ-theory), which is still the most often used technique because it has the advantage of a straightforward control mechanism, is particularly close to the time domain [11], [14, 15]. Their control mechanisms, however, are quite stiff, limiting their flexibility to be immediately implemented in varied power system setups. For example, the constant instantaneous power control strategy cannot enable the compensated current to be pure sinusoidal under voltage distortions. To produce a sinusoidal current, constant power must be obtained from the utility that is meant to utilize the constant instantaneous power control strategy [16]. So, based on this control strategy, the SAPF should compensate all harmonics in the current, but because the supply voltage primarily contains positive sequence harmonics, it may also contain negative sequence and zero sequence harmonics, a positive-sequence detector is required in the filter to extract the amplitude, phase angle, and frequency of the fundamental positive-sequence voltage and provide it in the form of instantaneous voltage. By adding the positive-sequence detector to the PQ-theory, the controller becomes able to avoid source voltage distortions and the controller is called the sinusoidal source current control strategy (Sinusoidal PQ-theory). The positive-sequence voltage detector which is necessary and based on dual active-reactive power (PQ) control theory depending on an important part of the Phase Locked Loop (PLL) circuit, the complete functional control block diagrams for overall control technique, positive-sequence voltage detector, and PLL circuit are shown in **Fig. 2**, **Fig. 3**, and **Fig. 4** respectively [16-19].

2.2. Hysteresis Band Current Control (HBCC)

The Current signals obtained by the Sinusoidal PQ-theory controller $i_{C a,b,c}^*$ and the actual injected currents $I_{C a,b,c}$ are given to the HBCC for generating the VSI necessary gating signals. **Figure 5** shows the control phenomenon, where the output signals of the HBCC are the input pulses to the six switches (S1-6) of the VSI [20].



3. LITERATURE REVIEW AND PAPER CONTRIBUTION

Harmonic mitigation is handled by the PI-controllers found in Sinusoidal PQ-theory and PLL circuits, so, the gains of PI-controllers K_p and K_i levels must be carefully optimized. The traditional approach of setting the PI-controller gains requires linear modeling, which results in non-optimal gain tuning [21, 22]. For PI-controller tuning, many metaheuristic optimization techniques are applied. Many control strategies exist to decrease current harmonics and offer additional capabilities to the converter [23]. particle swarm optimization (PSO) [24-26], simulated annealing (SA), Atom Search Optimization (ASO) [27], and genetic algorithm (GA) [28] are a few examples. Recently, new, and updated optimization algorithms have been implemented for the same reason; however, the purpose of this article is to introduce reliable and efficient techniques to meet the target and attain the desired objective function when compared to previous methods.

The reference current in this study is created using Sinusoidal PQ-theory based on the instantaneous active and reactive power theory (PQ-theory). The needed gating pulses are calculated using the Hysteresis Band Current Controller (HBCC) technique [29]. In sinusoidal PQ- theory, the PI-controllers for the PLL circuit and dc-link voltage must fine-tune their gain values, k_p , and k_i . Furthermore, the motivation for this article is based on a Mayfly Optimization Algorithm (MOA) that was proposed and tested against other previously and recently proposed algorithms such as (PSO), Artificial Hummingbird Algorithm (AHA), Archimedes Optimization Algorithm (AOA) to obtain optimized PI-controller gain values and the objective function with THD minimization, and the performance of the optimized controller is evaluated under variable load and distorted source voltage.

4. MAYFLY OPTIMIZATION ALGORITHM (MOA)

4.1. Definition

The MOA is an enhanced optimization algorithm. It combines the benefits of the PSO [30], GA [31], and firefly algorithm (FA) [32] to provide a strong hybrid algorithm framework. The crossover technique and local search are employed based on the mayfly's social behaviors. By Assumption, after hatching the mayfly will always be an adult, and the strongest mayfly will survive. Each mayfly's location in the search space symbolizes a possible solution [33].

4.2. MOA Principal of Operation

The performance of the proposed solution which is represented by the n-dimensional vector $x = (x_1, x_2, \dots, x_n)$, which is made up of two swarms of mayflies, females, and males, is assessed using the pre-set objective function $f(x)$. The change in the mayfly's position is represented by a speed vector $v = (v_1, v_2, \dots, v_d)$. Each mayfly's flight path is the result of a dynamic interplay between their personal and communal flying experiences. The mayfly will specifically alter its course each time to obtain its personal best location, which is the best location attained by every mayfly in the swarm [34].

4.3. Flow Chart of MOA

The steps of implementation of the MOA are clearly described by the flow chart shown in **fig.6**, Where g_{best} is the global optimal solution, and p_{best} is the optimal location or position that mayfly has never reached [35].

5. PROBLEM DEFINITION AND OBJECTIVE FUNCTION

The objective function of the Algorithms is to minimize the total Harmonic distortion THD of the source current. To do it, the PI-Controllers gains are tuned and optimized by the proposed optimization algorithms as illustrated in **Fig. 7**.

The THD is defined as the ratio of the RMS value of the total of all harmonic components up to a certain order to the RMS value of the fundamental component and can be expressed as in Eq. (1) [7, 13]. Where the gains are responding to the error and steady-state error respectively.

DYNAMIC PERFORMANCE OPTIMIZATION OF SHUNT ACTIVE POWER FILTER TO ELIMINATE TOTAL HARMONIC DISTORTION

The PI-controller transfer function is expressed as in Eq. (2), while the PI-controller output $u(t)$ is given as in Eq. (3).

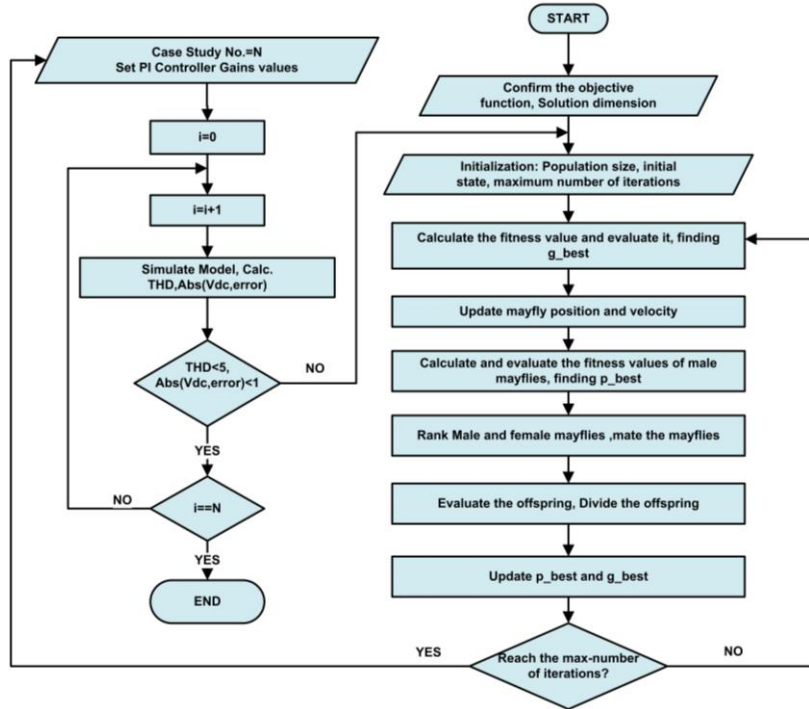
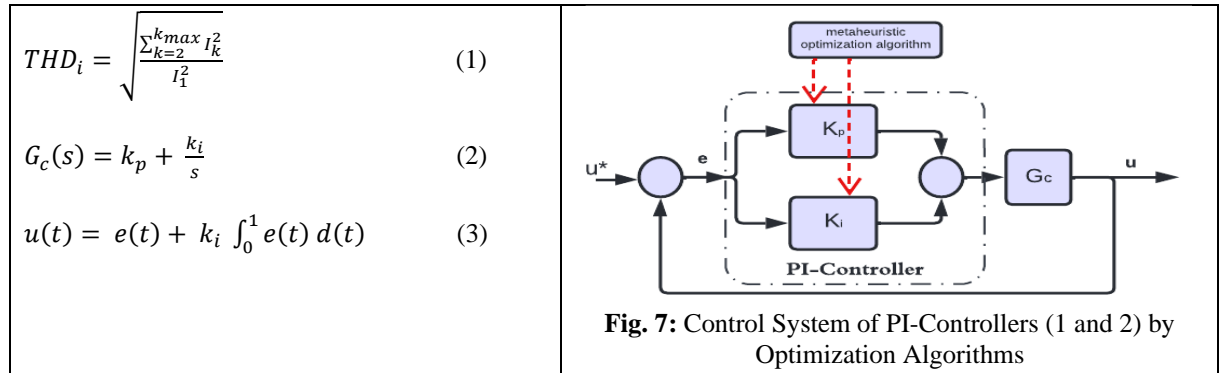


Fig. 6: Flow chart of the proposed algorithm (MOA)



where, $e(t)$ is the error between the actual value (u) and the reference Value (u^*) [34].

6. MODEL CONFIGURATION

The proposed model configuration is illustrated in **Fig. 8**, it contains a three-phase power grid connected to a three-phase un-controlled diode full bridge rectifier connected with an inductive load on the DC side which represent the non-linear load. At the PCC, SAPF with VSI design and capacitor on the DC link bus is integrated with the network.

The DC side capacitor reference voltage ($V_{dc,ref}$) is calculated as in Eq. 4, and the DC side capacitance (C_{dc}) value is calculated as in Eq. 5 [22].

$$V_{dc,ref} = \frac{2\sqrt{2}V_{LL}}{\sqrt{3}m} \quad (4)$$

$$\frac{1}{2} C_{dc}(V_{dc,ref}^2 - V_{dc}^2) = 3(V_s)(aI)(t) \quad (5)$$

Where, (V_{LL}) is AC line voltage, (m) is the modulation index, (a) is the factor of over-loading chosen as 1.2, (V_s) is the source voltage, (I) is the phase current, and (t) is the recovery time of DC-bus voltage. The parameters of the model are listed in **Table 1**.

DYNAMIC PERFORMANCE OPTIMIZATION OF SHUNT ACTIVE POWER FILTER TO ELIMINATE TOTAL HARMONIC DISTORTION

Table 1. Proposed System Parameters

System Parameters		Values
Supply Parameters	Voltage V_s	380 V
	Frequency f_s	50 Hz
	Source line resistor R_s	5 Ω
	Source line inductor L_s	2 mH
Non-Linear Load (6-Diodes Rectifier)	Load resistor R_{dc}	40 Ω
	Load resistor R_{dc}	30 mH
	Inductor L_{dc}	
Shunt Active Power Filter (SAPF)	Interface Resistor R_f	1 Ω
	Interface Inductor L_f	3 mH
	DC side Capacitor C_{dc}	1.8 mF
	References	650 V
	Voltage $V_{dc,ref}$	

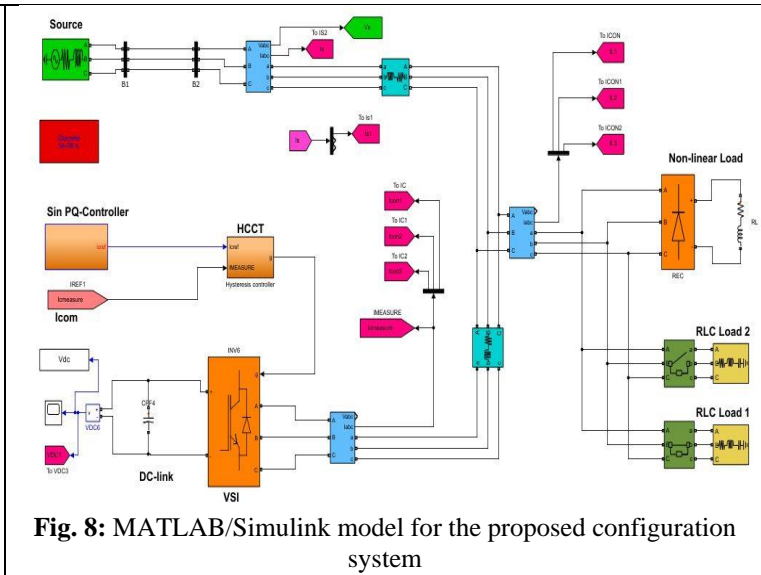


Fig. 8: MATLAB/Simulink model for the proposed configuration system

7. SIMULATION RESULTS AND DISCUSSION

The simulation and obtained results are carried out in MATLAB/SIMULINK environment. The initialization data for the proposed algorithms (PSO, AHA, AOA, and MOA) are listed in **Table 2**.

Table 2. Initialization Data for Proposed Optimization Algorithms

No. of Variables	Variables Upper / Lower Limits				Objective function	Population Number	Max. Iteration Number
	PI-Controller (1) gains		PI-Controller (2) gains				
4	$50 < K_{p1} < 250$	$1 < K_{i1} < 15$	$50 < K_{p2} < 250$	$1 < K_{i2} < 15$	THD _i	10	200

7.1. Simulation Scenarios

In this section, the gains of the PI-controller are optimized to improve the value of the source current THD. Then, the performance of the controller is evaluated under the static non-linear load connected at the PCC. This evaluation was implemented according to the following scenarios.

- Scenario 1. Without connected SAPF.
- Scenario 2. With connected SAPF without PI-controller tuning.
- Scenario 3. With connected SAPF and PI-controller tuned by PSO.
- Scenario 4. With connected SAPF and PI-controller tuned by AHA.
- Scenario 5. With connected SAPF and PI-controller tuned by AOA.
- Scenario 6. With connected SAPF and PI-controller tuned by MOA.

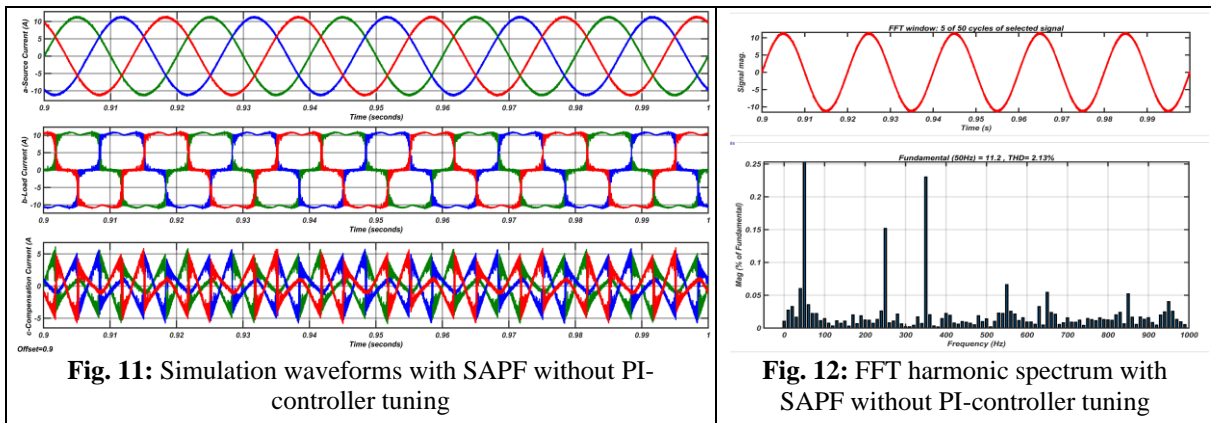
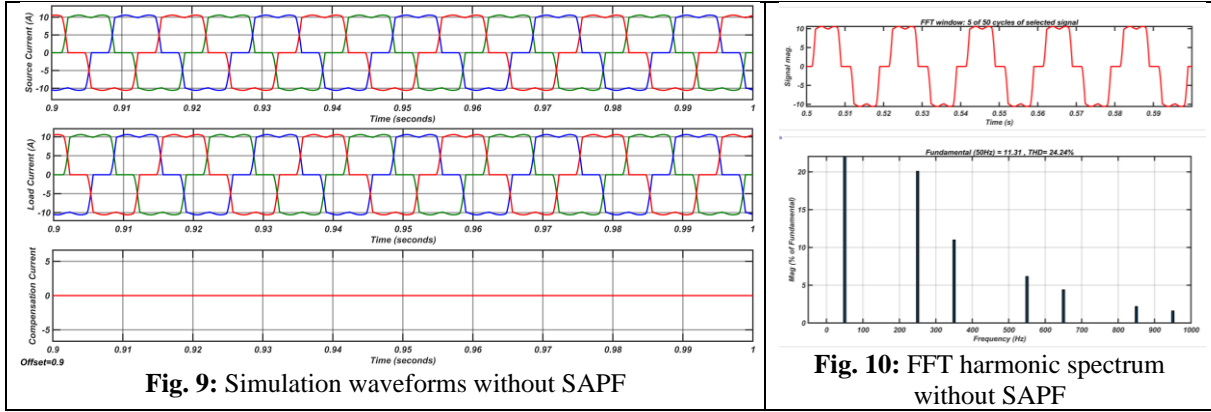
7.1.1. Scenario 1: without connected SAPF.

In this case, SAPF is disconnected and the distortion in source current caused by the nonlinear load is obtained by Fast Fourier Transform (FFT) analysis which calculated about 24.24%. **Figure 9** shows the three-phase simulation waveforms for source and load currents. **Figure 10** shows FFT harmonic spectrum for the source current.

7.1.2. Scenario 2: With connected SAPF without PI-controller tuning.

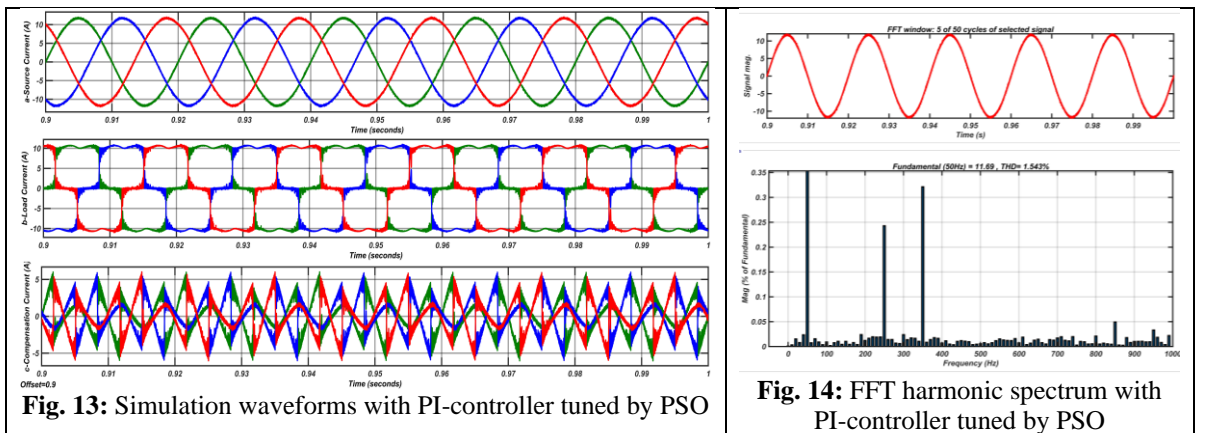
In this case, SAPF is connected at PCC, the simulation results are taken without tuning of PI-controller gains. The distortion in supply current distortion after SAPF compensation is reduced and becomes 2.13%. The simulation waveforms for the source current, load current, and compensating filter current are shown in **Fig.11**. And the harmonic spectrum for the source current is shown respectively in **Fig.12**.

DYNAMIC PERFORMANCE OPTIMIZATION OF SHUNT ACTIVE POWER FILTER TO ELIMINATE TOTAL HARMONIC DISTORTION



7.1.3. Scenario 3: With connected SAPF and PI-controller tuned by PSO.

In this case, the simulation operated with SAPF compensation action, and PI-controller gains are tuned by PSO Algorithm. The obtained results indicate that the THD for the source current is reduced to 1.543% when $K_{p1}=72.75$, $K_{i1}=4.50$, $K_{p2}=63.35$, and $K_{i2}=5.96$. **Figure 13** shows waveforms of the source current, load current, and the compensating SAPF current. **Figure 14** shows the harmonic spectrum for the source current.



7.1.4. Scenario 4: With connected SAPF and PI-controller tuned by AHA.

The obtained results with the AHA algorithm indicate that the THD is reduced to 1.546% when $K_{p1}=99.16$, $K_{i1}=9.9$, $K_{p2}=54.97$, and $K_{i2}=2.66$. **Figure 15** shows simulation waveforms for all source, load, and compensating currents. **Figure 16** shows the source current THDi harmonic spectrum.

DYNAMIC PERFORMANCE OPTIMIZATION OF SHUNT ACTIVE POWER FILTER TO ELIMINATE TOTAL HARMONIC DISTORTION

7.1.5. Scenario 5: With connected SAPF and PI-controller tuned by AOA.

Distortion for supply current signal is decreased to 1.547% when $K_{p1}=203.13$, $K_{i1}=6.55$, $K_{p2}=67.94$, and $K_{i2}=7.09$ when tuning PI-controller using the AOA algorithm. The waveforms for all current signals are shown in **Fig. 17**. And THD harmonic spectrum value obtained by FFT is shown in **Fig. 18**.

7.1.6. Scenario 6: With connected SAPF and PI-controller tuned by MOA

PI-controller gains are tuned using the MOA algorithm and the best fitness (minimized THD) is mitigated to 1.531% when $K_{p1}=203.52$, $K_{i1}=1$, $K_{p2}=57.85$, and $K_{i2}=1$. **Figure 19** shows the source current, load current, and compensating current waveforms. **Figure 20** shows the THD spectrum for the drawn supply current.

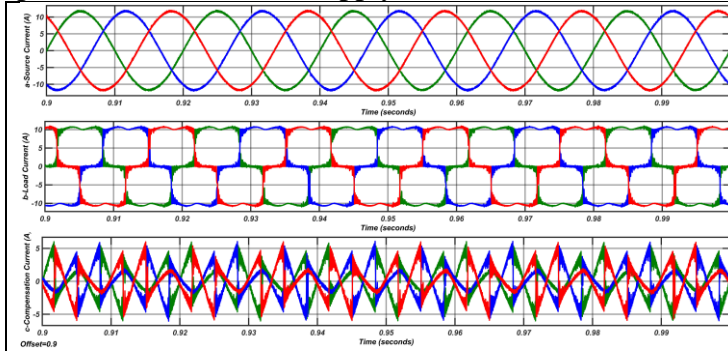


Fig. 15: Simulation waveforms with PI-controller tuned by AHA

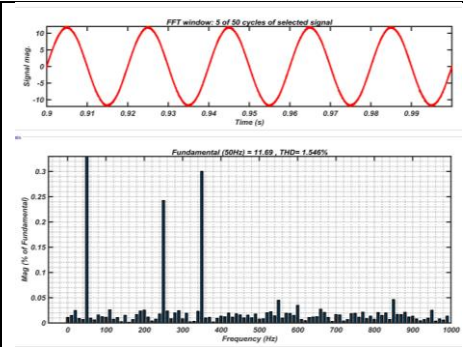


Fig. 16: FFT harmonic spectrum with PI-controller tuned by AHA

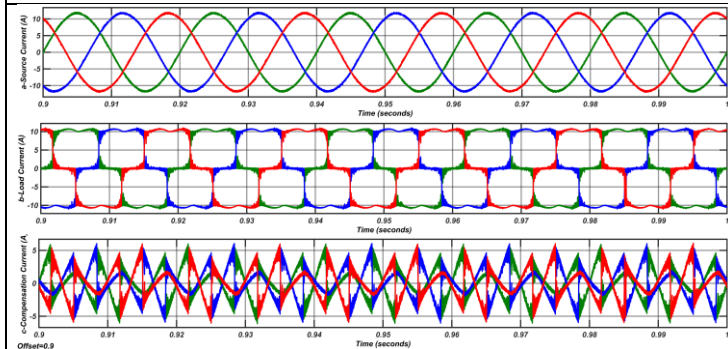


Fig. 17: Simulation waveforms with PI-controller tuned by AOA

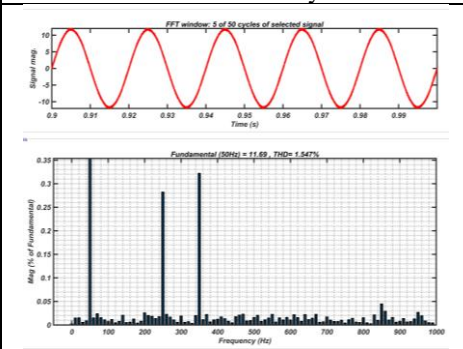


Fig. 18: FFT harmonic spectrum with PI-controller tuned by AOA

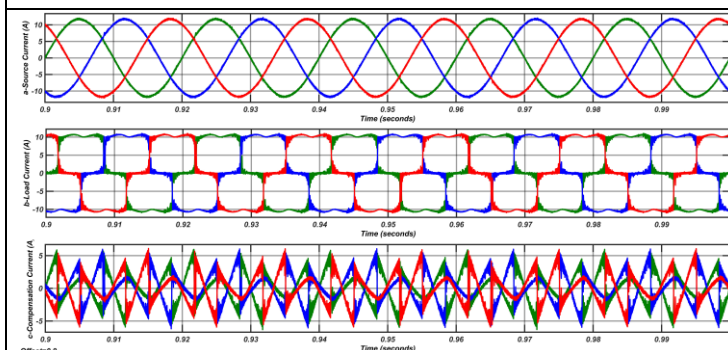


Fig. 19: Simulation waveforms with PI-controller tuned by MOA

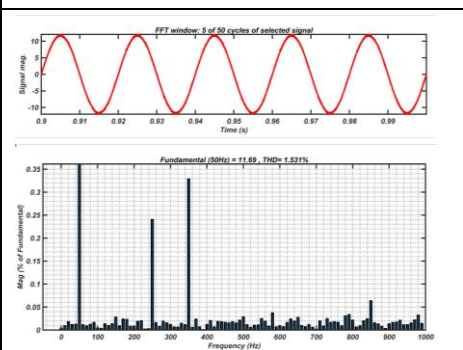


Fig. 20: FFT harmonic spectrum with PI-controller tuned by MOA

7.2. Comparison Between the Optimized Results for all suggested Algorithms

As shown in **Table 3** and **Fig. 21**, the performance of the SAPF is improved clearly with MOA tuning PI-controller and based on the optimized gains the minimization of the THD objective function is obtained and its best fitness value becomes 1.531% which is the least value compared with values obtained from other algorithms, and it converged at 138 iterations which is the most continuous improvement.

DYNAMIC PERFORMANCE OPTIMIZATION OF SHUNT ACTIVE POWER FILTER TO ELIMINATE TOTAL HARMONIC DISTORTION

Figure 22 illustrates the speed and accuracy of DC-link voltages for matching the reference value for the suggested algorithms used. It shows that the MOA is the fastest and closest to the reference value with accepted settling time, dc-link voltage overshoot, and steady-state error which attain more enhancement for SAPF controller performance.

Table 3. Control Parameters, THD fitness, and Convergence iteration results for the proposed Algorithms

Proposed tuning Algorithm	Best of fitness (THD _i)	Best solutions				Convergence iteration
		K _{p1}	K _{i1}	K _{p2}	K _{i2}	
PI-Controller without tuning	2.229%	1	1	1	1	--
PI-Controller tuned by PSO	1.543%	72.75	4.5	63.35	5.96	92
PI-Controller tuned by AHA	1.546%	99.16	9.9	54.97	2.66	123
PI-Controller tuned by AOA	1.547%	203.13	6.55	67.94	7.09	54
PI-Controller tuned by MOA	1.531%	203.52	1	57.85	1	138

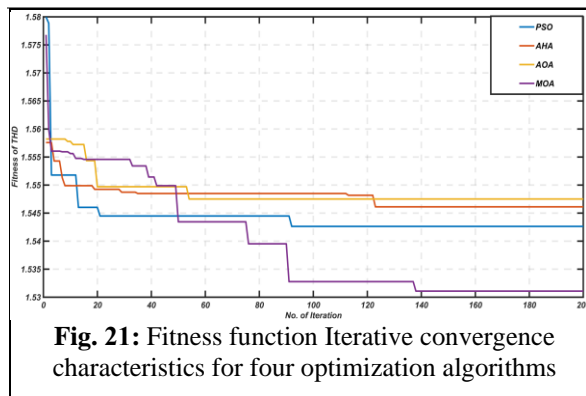


Fig. 21: Fitness function iterative convergence characteristics for four optimization algorithms

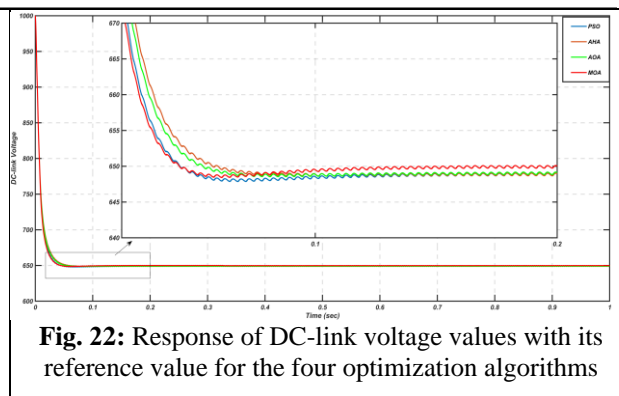


Fig. 22: Response of DC-link voltage values with its reference value for the four optimization algorithms

7.3. Performance Evaluation of The Optimized Controller Under Variable Load Conditions

In this section, the performance of the optimized controller which is tuned using the MOA is evaluated under dynamic conditions. In addition to the non-linear load, which is connected at the PCC, double three-phase RLC loads are connected to the PCC with double three-phase circuit breakers. Each load has a power capacity equal to one-half of the non-linear load. One of these breakers switches off/on at times 0.6 sec. and 0.8 sec. and the other breaker switches on at a time of 0.4 sec. So, the simulation time is divided into three intervals:

- [1] ($0 \leq t \leq 0.6$ sec), the connected load consists of the non-linear load with a single RLC load.
- [2] ($0.6 \leq t \leq 0.8$ sec), the connected load only consists of the non-linear load.
- [3] ($0.8 \leq t \leq 1$ sec), the connected load consists of the non-linear load with double RLC loads.

The source current, load current, and compensation current waveforms under variable load conditions are shown in **fig. 23** for all intervals.

By using the FFT analysis, the THD of the source current was calculated under variable load conditions to evaluate the performance of the optimized gain controller. **Table 4** illustrates the THD of the source current over all intervals. This is obtained using the controller when its gains are tuned by the MOA.

For a better evaluation of the control performance, it is necessary to study the response of the DC-link voltage under dynamic condition, so **Fig. 24** represent the dynamic response of the DC-link voltage value concerning its reference value under variable load condition for the MOA algorithm. Also, it shows that the MOA is always controlled by the DC-link voltage close to the reference value with minimum steady state error which attains more enhancements for SAPF controller performance.

DYNAMIC PERFORMANCE OPTIMIZATION OF SHUNT ACTIVE POWER FILTER TO ELIMINATE TOTAL HARMONIC DISTORTION

Table 4. THD under variable load condition			
Proposed tuning Algorithm	THD%		
	$0 \leq t \leq 0.6$	$0.6 \leq t \leq 0.8$	$0.8 \leq t \leq 1$
Without SAPF	17.921	24.24	14.641
PI-Controller tuned by MOA	0.829	1.531	0.381

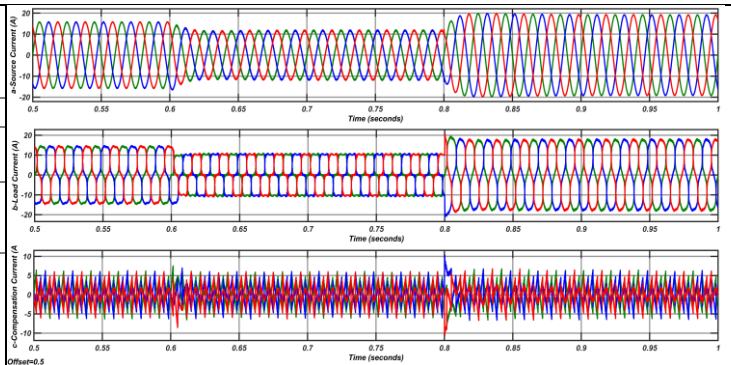
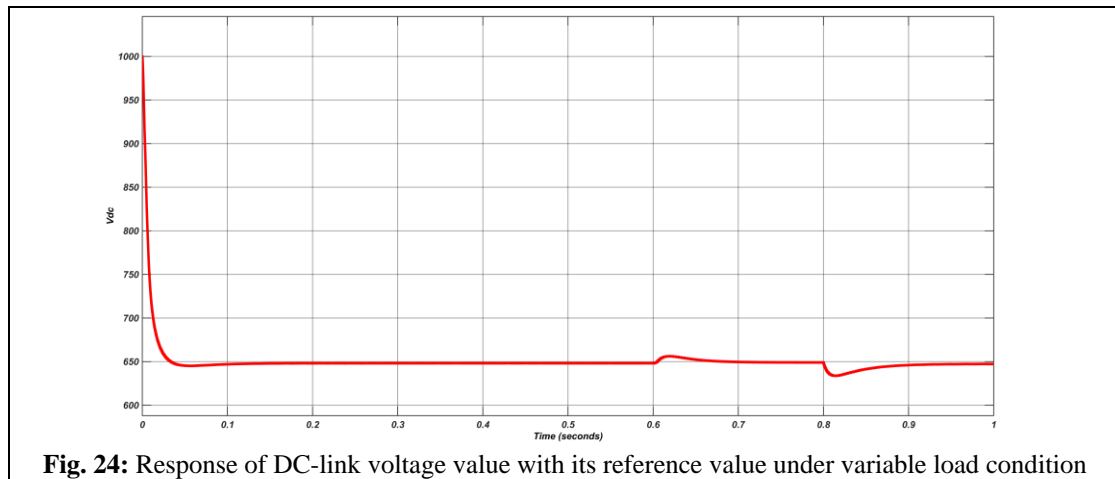
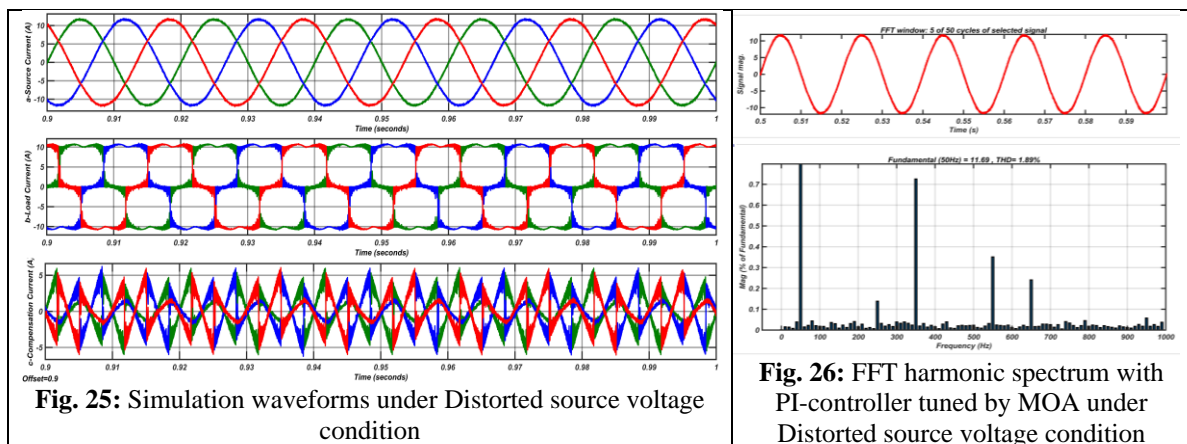


Fig. 23: Simulation waveforms under variable load conditions



7.4. Performance Evaluation of The Optimized Controller Under Distorted Source Voltage Condition

The strong and distinctive performance of the controller appears when it is tested and evaluated with distortions in the source voltage waveform. When the source voltage has distorted by 5.3%, the THD for the source current is maintained within permissible value by the SAPF which is controlled by the proposed controller. **Figure 25** shows the source current, load current, and compensating current waveforms. Where the THD value is 1.89%. **Figure 26** shows the THD spectrum for the drawn supply current.



8. CONCLUSION

In this proposed system a SAPF controller applied a Mayfly Optimization Algorithm (MOA) to optimize the PI-controllers gain values which placed at PLL circuit and the dc-link voltage regulator in sinusoidal PQ-theory. The controller optimized by the MOA is tested with simulation and compared with the other optimization algorithms. The suggested MOA algorithm provides better performance and introduces a better accuracy due to the optimized output parameters for SAPF like THD of the source current, settling time, steady state error of dc-link voltage, and peak overshoot.

The succeeding conclusions have been ended from the previous study:

1. Effectively compensate for 24.24%. THD due to current harmonics and reactive power generated by non-linear load and the purposed controller technique mitigates the supply current THD well within acceptable and standard value below 5% and the source current becomes sinusoidal.
2. With all tuning PI-controller optimization methods, all THD values are less than the value obtained without PI-controller tuning, and DC-link capacitor voltage returns its reference value without any deviation against the conventional PI-controller.
3. MOA outperforms a great, most accurate performance, and best correlation dc-link voltage reference voltage compared to other PSO, AHA, and AOA algorithms, and gives a minimum THD value of 1.531% for the source current.
4. Also, under variable load conditions, MOA gives acceptable results over all three intervals, where the THD values are 0.829%, 1.531%, and 0.381% respectively. In addition, it gives a great performance in DC-link voltage response under dynamic conditions.
5. Under distorted source voltage, the MOA gives good results, where the THD value is 1.89%.

REFERENCES

- [1] Institute of Electrical and Electronics Engineers. (2014). IEEE recommended practice and requirements for harmonic control in electric power systems. IEEE.
- [2] Soni, M. K., & Soni, N. (2014). Review of causes and effect of harmonics on power system. *International Journal of Science, Engineering and Technology Research*, 3(2), 214-220.
- [3] Hannan, M. A., Islam, N. N., Mohamed, A., Lipu, M. S. H., Ker, P. J., Rashid, M. M., & Shareef, H. (2018). Artificial intelligent based damping controller optimization for the multi-machine power system: A review. *IEEE Access*, 6, 39574-39594.
- [4] Jajarmi, H. I., Mohamed, A., & Shareef, H. (2014). Adaptive interval type2 fuzzy hysteresis-band current-controlled active power filter for power quality improvement. *Przegląd Elektrotechniczny*, 90(9), 140-145.
- [5] Hoon, Y., Mohd Radzi, M. A., Mohd Zainuri, M. A. A., & Zawawi, M. A. M. (2019). Shunt active power filter: A review on phase synchronization control techniques. *Electronics*, 8(7), 791.
- [6] Imani, H. R., Mohamed, A., Shareef, H., & Eslami, M. (2013). Multi-objective optimization based approaches for active power filter design-A comparison. *Przegląd Elektrotechniczny*, 89(6), 98-103.
- [7] Kazemzadeh, R., Najafi Aghdam, E., Fallah, M., & Hashemi, Y. (2014). Performance scrutiny of two control schemes based on DSM and HB in active power filter. *Journal of Operation and Automation in Power Engineering*, 2(2), 103-112.
- [8] Al-Ogaili, A. S., Ramasamy, A., Hoon, Y., Verayiah, R., Marsadek, M., Juhana, T., & Rahmat, N. A. (2020). Time-domain harmonic extraction algorithms for three-level inverter-based shunt active power filter under steady-state and dynamic-state conditions-an evaluation study. *International Journal of Electrical & Computer Engineering* (2088-8708), 10(6).
- [9] Monfared, M., Golestan, S., & Guerrero, J. M. (2013). A new synchronous reference frame-based method for single-phase shunt active power filters. *Journal of power Electronics*, 13(4), 692-700.
- [10] Akagi, H., Watanabe, E. H., & Aredes, M. (2017). *Instantaneous power theory and applications to power conditioning*. John Wiley & Sons.

DYNAMIC PERFORMANCE OPTIMIZATION OF SHUNT ACTIVE POWER FILTER TO ELIMINATE TOTAL HARMONIC DISTORTION

- [11] Eskandarian, N., Beromi, Y. A., & Farhangi, S. (2014). Improvement of dynamic behavior of shunt active power filter using fuzzy instantaneous power theory. *Journal of power Electronics*, 14(6), 1303-1313.
- [12] Hoon, Y., Mohd Radzi, M. A., Hassan, M. K., & Mailah, N. F. (2017). Control algorithms of shunt active power filter for harmonics mitigation: A review. *Energies*, 10(12), 2038.
- [13] AttiyaSoliman, A. M., Kandil, T. A., Mehanna, M. A., & EL-Sayed, S. K. (2014). Mitigation of the Effect of HVDC System on Power System Quality at Distribution Level. Department of Electrical Power and Machines, Faculty of Engineering, Al-Azhar University, Egypt,(IJEIT) Volume, 4.
- [14] Hoon, Y., Mohd Radzi, M. A., Hassan, M. K., & Mailah, N. F. (2018). A dual-function instantaneous power theory for operation of three-level neutral-point-clamped inverter-based shunt active power filter. *Energies*, 11(6), 1592.
- [15] Imam, A. A., Sreerama Kumar, R., & Al-Turki, Y. A. (2020). Modeling and simulation of a PI controlled shunt active power filter for power quality enhancement based on PQ theory. *Electronics*, 9(4), 637.
- [16] Monteiro, L. F., & Aredes, M. (2002, July). A comparative analysis among different control strategies for shunt active filters. In Proc.(CDROM) of the V INDUSCON-Conferência de Aplicações Industriais, Salvador, Brazil (pp. 345-350).
- [17] Soliman, A. M. A., El-Sayed, S. K., & Mehanna, M. A. (2017). Effect of Utility Voltage Distortion on the Performance of Different Control Strategies for Shunt Active Power Filter. *European Journal of Engineering and Technology Research*, 2(8), 27-34.
- [18] Eid, A.A., Soliman, A. M. A., & Mehanna, M. A. (2022). Optimize Gain Values of PI-Controller for Active Power Filter Using Mayfly Algorithm. *International Journal of Renewable Energy Research (IJRER)* Vol.12, No.4.
- [19] Zabihi, N., & Gouws, R. (2014). Analysing two control methods of shunt active filters for unbalanced load.
- [20] Storn, R., & Price, K. (1997). Differential evolution—a simple and efficient heuristic for global optimization over continuous spaces. *Journal of global optimization*, 11(4), 341-359.
- [21] Sao, J. K., Naayagi, R. T., Panda, G., Patidar, R. D., & Swain, S. D. (2022). SAPF Parameter Optimization with the Application of Taguchi SNR Method. *Electronics*, 11(3), 348.
- [22] Acharya, D. P., Choudhury, S., & Nayak, N. (2022). Optimal Design of Shunt Active Power Filter for Power Quality Improvement and Reactive Power Management Using nm-Predator Prey Based Firefly Algorithm. *International Journal of Renewable Energy Research (IJRER)*, 12(1), 383-397.
- [23] Babu, B. M., Srinivas, L. R., & Ram, S. T. (2018). Power quality improvement based on PSO algorithm incorporating UPQC. *Journal of Engineering and Technology*, 9(1), 1-16.
- [24] Avila, V. H., & Leite, V. (2020, September). Control of grid-connected inverter output current: A practical review. In 2020 9th International Conference on Renewable Energy Research and Application (ICRERA) (pp. 232-235). IEEE.
- [25] Bangia, S., Sharma, P. R., & Garg, M. (2013, February). Comparison of artificial intelligence techniques for the enhancement of power quality. In 2013 International Conference on Power, Energy and Control (ICPEC) (pp. 537-541). IEEE.
- [26] Vadi, S., Gurbuz, F. B., Sagioglu, S., & Bayindir, R. (2021, June). Optimization of pi based buck-boost converter by particle swarm optimization algorithm. In 2021 9th International Conference on Smart Grid (icSmartGrid) (pp. 295-301). IEEE.
- [27] Oymak, A., & Tur, M. R. (2022). A Short Review on the Optimization Methods Using for Distributed Generation Planning. *International Journal of Smart Grid-ijSmartGrid*, 6(3), 54-64.
- [28] Rao, G. S., Goud, B. S., & Reddy, C. R. (2021, June). Power Quality Improvement using ASO Technique. In 2021 9th International Conference on Smart Grid (icSmartGrid) (pp. 238-242). IEEE.
- [29] Karuppanan, P. (2012). Design and Implementation of Shunt Active Power Line Conditioner using Novel Control Strategies (Doctoral dissertation).
- [30] Wang, C., Ping, D., Song, B., & Zhang, H. (2021). Optimization of multi-machine passive positioning system based on PSO. *Comp. Digital Eng*, 49, 487-492.
- [31] Höschel, K., & Lakshminarayanan, V. (2019). Genetic algorithms for lens design: a review. *Journal of*

**DYNAMIC PERFORMANCE OPTIMIZATION OF SHUNT ACTIVE POWER FILTER TO ELIMINATE
TOTAL HARMONIC DISTORTION**

Optics, 48(1), 134-144.

- [32] Yang, X. S., & He, X. (2013). Firefly algorithm: recent advances and applications. arXiv preprint arXiv:1308.3898.
- [33] Hu, A., Deng, Z., Yang, H., Zhang, Y., Gao, Y., & Zhao, D. (2021). An Optimal Geometry Configuration Algorithm of Hybrid Semi-Passive Location System Based on Mayfly Optimization Algorithm. *Sensors*, 21(22), 7484.
- [34] Shamaei, K., Khalife, J., & Kassas, Z. M. (2018). Exploiting LTE signals for navigation: Theory to implementation. *IEEE Transactions on Wireless Communications*, 17(4), 2173-2189.
- [35] Durmus, A., Kurban, R., & Karakose, E. (2021). A comparison of swarm-based optimization algorithms in linear antenna array synthesis. *Journal of Computational Electronics*, 20(4), 1520-1531.